Microsystem Technologies
https://doi.org/10.1007/s00542-019-04616-8

TECHNICAL PAPER

High-selectivity adjustable dual-band bandpass filter using a quantic-mode resonator

Kai Li[1] · Guo-qin Kang[1] · Han Liu[1] · Zhi-yuan Zhao[1]

Received: 3 July 2019 / Accepted: 3 September 2019

Abstract
A novel adjustable dual-band bandpass filter using a quantic-mode resonator consisting of stepped impedance resonators (SIRs) and coplanar waveguide resonators (CPWRs) is proposed in this paper. The SIRs provide the lower passband with two transmission poles (TPs), while the upper passband is introduced by CPWRs and two TPs are obtained. Furthermore, an equivalent rectangular loop resonator (RLR) derived from the CPWRs is also introduced, providing another TP for the upper passband. One of the marked features of the filter is that the two passbands can be adjusted independently because of the independent resonant paths of different resonators. Besides, this filter has four transmission zeros (TZs), promising good stopband rejection and high band-to-band isolation. The measured results are consistent with the simulated results.

1 Introduction

High-performance dual-band bandpass filters are widely used in multi-service communication systems (Chen and Chu 2016). The multi-mode technology and the hybrid technology are two mainstream methods to design the dual-band bandpass filters. The multi-mode technology is enabled by rectangular loop resonator (RLR) (Fu et al. 2012), patch resonator (Ieu et al. 2017), and stub-loaded resonator (You et al. 2014), etc. The hybrid technology is realized by the combination of substrate integrated waveguide (SIW) and coplanar waveguide (CPW) (Chu et al. 2014), patch resonator (Leu et al. 2018) and CPW (Duan et al. 2015), RLR and microstrip stubs (Ieu et al. 2017), etc. Compared with multi-mode technology, the hybrid technology enables a more compact circuit and the each mode of dual-band resonators can be tuned independently. Usually, every resonator of a hybrid resonator has an independent resonant path, and some experts have been studying it. An independently-tuned dual-band bandpass filter using hybrid structure, which consists of RLR and microstrip stubs, is proposed in Ieu et al. (2017), four TEM modes are excited with independent resonant paths through direct coupling (strong coupling) and microstrip dual-feed line weak coupling, while the hybrid structure seems sill too complex, moreover, its measurement results are not satisfactory (Khani et al. 2017). A compact microstrip dual-band bandpass filter with tunable center frequency, compact size and low insertion loss is proposed in Khani et al. (2018), while only the center frequency of the upper passband can be tuned. It's not unique, a narrow dual-band BPF with a fixed lower passband and an independently tunable upper passband is proposed in Mousavi et al. (2018).

In this paper, a novel adjustable dual-band bandpass filter with a simple layout is proposed and its configuration is shown in Fig. 1. Two stepped impedance resonators (SIRs), two CPWRs and an equivalent RLR composed of two orthogonal CPWRs constitute a quantic-mode resonator, which has a hybrid structure indeed. Each resonator has an independent resonant path, so the two passbands can be adjusted independently. Four transmission zeros (TZs) are also introduced, improving the stopband rejection and band-to-band isolation.

✉ Kai Li
18695845556@163.com

Guo-qin Kang
693440285@qq.com

Han Liu
lujiangliuhan@sina.com

Zhi-yuan Zhao
zhaozhiyuan1986@sina.com

[1] College of Information and Communication, National University of Defense Technology, Wuhan 430014, China

Published online: 06 September 2019

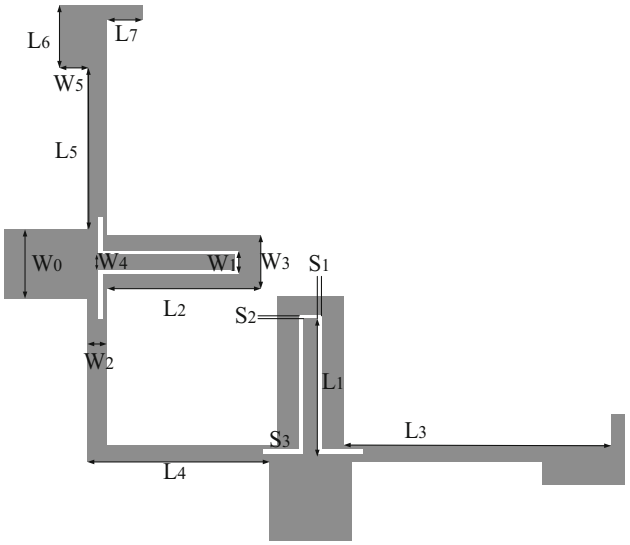

Fig. 1 Configuration of proposed dual-band bandpass filter

2 Analysis of the configuration of the filter

The proposed filter has five transmission poles (TPs) provided by a quantic-mode resonator, as shown in Fig. 2a. Each TP is obtained from a single equivalent resonator, and the layouts of all the resonators are illustrated in Fig. 2b–f respectively, while the E-field distributions of the five TPs and the corresponding resonant paths marked with the black arrows are all shown in Fig. 3a–e.

The resonator shown in Fig. 2f is derived from the two CPWRs and a rectangular loop resonator (RLR).

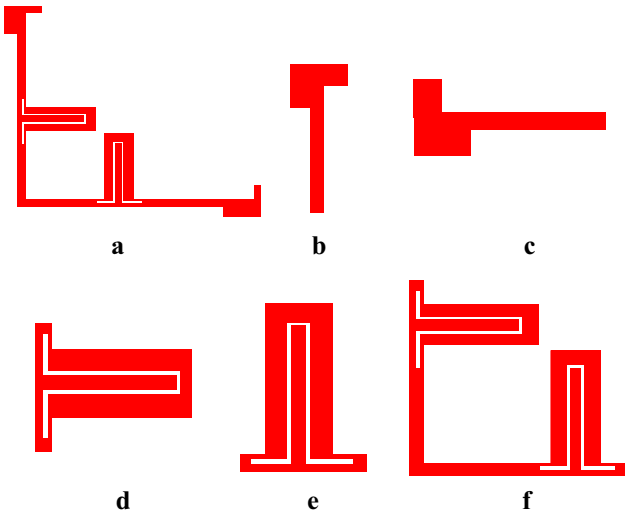

Fig. 2 Layouts of the resonators. **a** Quantic-mode resonator. **b** Resonator providing the first TP for the lower passband. **c** Resonator providing the second TP for the lower passband. **d** Resonator providing the first TP for the upper passband. **e** Resonator providing the second TP for the upper passband. **f** Resonator providing the third TP for the upper passband

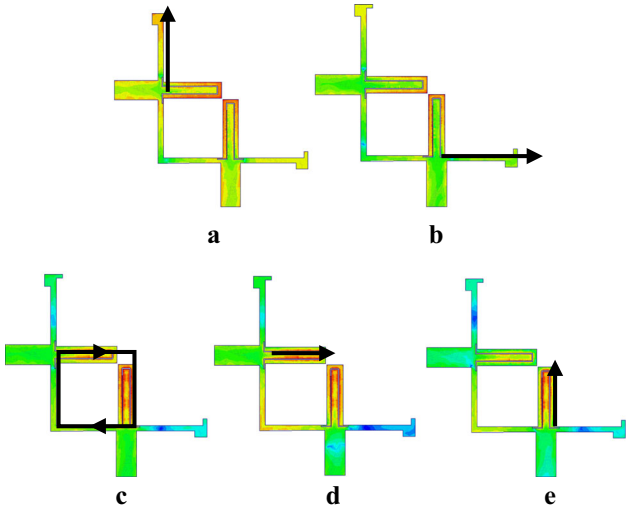

Fig. 3 E-field distributions at each TP. **a** At f = 2.28 GHz. **b** At f = 2.31 GHz. **c** At f = 3.12 GHz. **d** At f = 3.23 GHz. **e** At f = 3.35 GHz

Furthermore, the RLR can be analyzed with the odd/even mode method, and it has nearly the same resonant frequency with that of the CPWRs, as the CPWR is a 1/4 wavelength resonator and the two CPWRs are close to each other. The three resonators provide the upper passband with three TPs, while the two SIRs provide the lower passband with two TPs.

3 Analysis of the dual-band

As analyzed above, the two passbands can be adjusted independently since the five resonators have independent resonant paths.

The lower passband is adjusted by the length of the SIRs (L5 + L6 + L7), and the responses versus the length of the SIRs are shown in Fig. 4a. It follows that as the length of the SIR labelled with symbol L7 increases, the bandwidth of lower passband also increases, because the resonant frequency moves to lower end while the upper passband remains unchanged. Obviously, the bandwidth of lower passband is proportional to the length of SIR. An extra transmission path is introduced by the direct-connected orthogonal input and output port and it brings a TZ at the down stopband while another TZ is introduced by the cross coupling in quantic-mode resonator for the lower passband.

The length of CPWR (RLR) determines the upper passband, and an example of adjustable passband is shown in Fig. 4b. It can be concluded that as the length of CPWR labelled with symbol L1 decreases, the bandwidth of upper passband will increase, because the resonant frequency of CPWR moves to higher end while the bandwidth of the

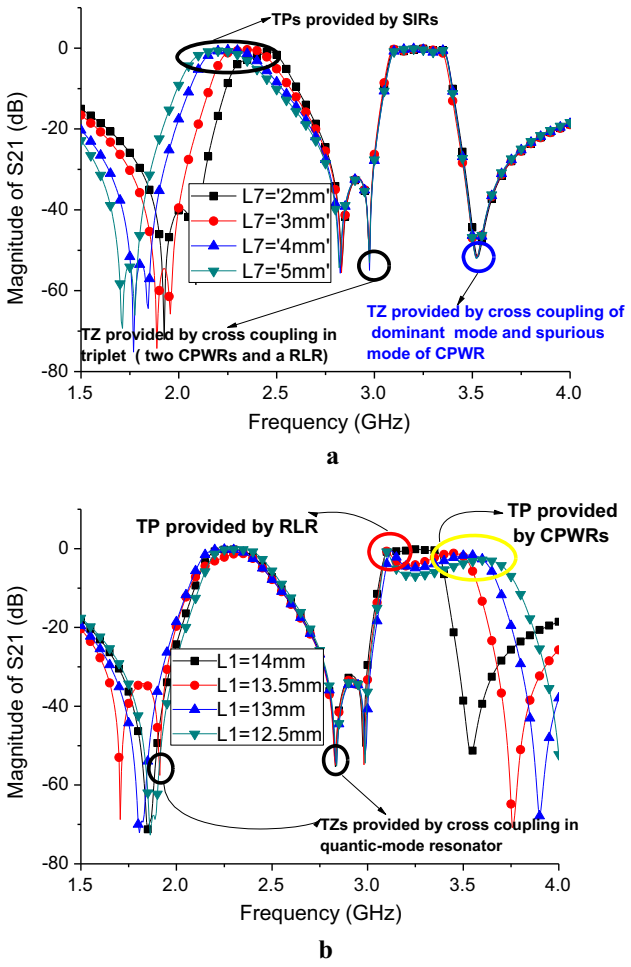

Fig. 4 Responses versus different parameters. **a** Lower passband changes with L7. **b** Upper passband changes with L1

lower passband remains unchanged. Figure 4b shows that the TP provided by the RLR is also not disturbed by the L1, and it is the key to adjusting the CPWR and RLR independently. The cross coupling between dominant mode and spurious mode of CPWR brings the upper passband a TZ at the upper stopband, while the cross coupling in a triplet (including two CPWRs and a RLR) and cross coupling in quantic-mode resonator generate two TZs between the two passbands.

Finally, the design processes of the proposed BPF are outlined as follows.

1. Figure out the design parameters according to the target specifications of the project.
2. Determine the synthetic matrix of upper passband M^{I}, the synthetic matrix of lower passband M^{II}, according to the design parameters and generalized Chebyshev synthesis, then determine the internal and external coupling coefficients.
3. According to MI,II i,l, specify the center frequencies, that is, the degree of offset relative to the center frequency of each passband.
4. Determine the initial size of each resonator by using the center frequency and optimized parameters.
5. Adjust the feeding position, control its external coupling coefficient, and the target value is matched.
6. Adjust L7, L1 and other parameters, control internal coupling (i.e., bandwidth), and match the target value.
7. Adjust filter parameters to optimize the performance and structure size.

4 Measurement

This dual-band bandpass filter using Rogers RT/duroid 5880, which is 0.254 mm in thickness and has a relative permittivity of 2.2, is simulated, fabricated and measured. The results are shown in Fig. 5. The dimensions of this dual-band bandpass filter are listed as follows: L1 = 14.2, L2 = 15.0, L3 = 16.9, L4 = 15.3, L5 = 14.5, L6 = 3.0, L7 = 1.6, W0 = 4.5, W1 = 2.1, W2 = 1.4, W3 = 4.1, W4 = 1.7, W5 = 1.5, S1 = 0.3 mm, S1 = 0.2, S2 = 1.4, S3 = 0.5 (all in millimeters). As illustrated in Fig. 5, the two passbands are centered at 2.3 GHz and 3.2 GHz, and the 3-dB fractional bandwidths (FBW) of them are 11.3% and 9.4% respectively. A TZ is located at the lower stopband (1.9 GHz), and a TZ is located at the upper stopband (3.5 GHz), while two TZs are located at 2.8 GHz and 3.0 GHz, between the two passbands. The measured maximum insertion losses are 1.1 dB and 1.7 dB respectively. The band-to-band isolation between the two passbands is > 30 dB.

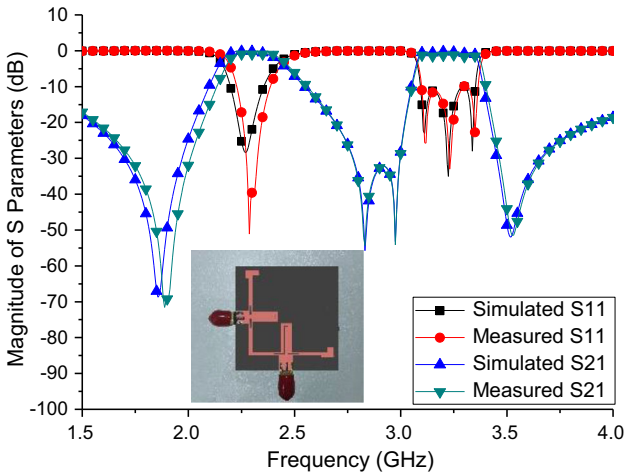

Fig. 5 Simulated and measured results of the proposed dual-band filter

Table 1 Comparisons between BPF proposed in this study and other proposed BPFs in the references (f_{01}: lower passband center frequency, f_{02}: upper passband center frequency, *IL* insertion loss, *RL* return loss, *TZ* transmission zero)

Refs.	f_{01} (GHz)	f_{02} (GHz)	IL_{01}/IL_{02} (dB)	RL_{01}/RL_{02} (dB)	Size (λ_g^2)	TZ number
Leu et al. (2018)	1.82	2.93	0.92/0.83	20/34	0.094	3
Ieu et al. (2017)	5.01	8.25	0.81/0.83	> 15/> 10	0.164	2
Khani et al. (2018)	2.4	5.7	0.22/0.56	27/23.8	0.012	0
Mousavi et al. (2018)	2.7	3.65–6.51	0.8/0.8–3.5	22/26–21	0.013	2
This work	2.3	3.2	1.1/1.7	> 40/> 12	0.228	4

Table 1 compares the proposed filter in this study with other proposed BPFs in some references, where f_{01} and f_{02} are the center frequencies in the lower and upper passband, IL_{01} and IL_{02} are insertion losses of respective band, RL_{01} and RL_{02} are return losses of respective band, where is the waveguide length at f_{01}.

5 Conclusion

A high-selectivity dual-band bandpass filter with independently adjustable passbands is proposed. The dual-band is obtained by a quantic-mode hybrid structure composed of five resonators, i.e., two CPWRs, two SIRs and an equivalent RLR derived from CPWRs. The resonant paths of SIRs are independent from that of CPWRs and RLR, so the passbands can be adjusted independently. Furthermore, five TPs are obtained while four TZs are introduced, improving the stopband rejection and band-to-band isolation.

References

Chen Z, Chu Q (2016) Dual-band reconfigurable bandpass filter with independently controlled passbands and constant absolute bandwidths. IEEE Microw Wirel Compon Lett 26(2):92–94

Chu P, Hong W, Dai L et al (2014) A planar bandpass filter implemented with a hybrid structure of substrate integrated waveguide and coplanar waveguide. IEEE Trans Microw Theory Tech 62(2):266–274

Duan Q, Song K, Chen F et al (2015) Compact dual-band bandpass filter using simply hybrid structures. Electron Lett 51(16):1265–1266

Fu S, Wu B, Chen J et al (2012) Novel second-order dual-mode dual-band filters using capacitance loaded square loop resonator. IEEE Trans Microw Theory Tech 60(3):477–483

Ieu W, Zhang D, Zhou D (2017a) High-selectivity dual-mode dual-band microstrip bandpass filter with multi-transmission zeros. Electron Lett 53(7):482–484

Ieu W, Zhou D, Zhang D, Han S (2017b) Dual-band bandpass filter using loop resonator with independently-tunable passband. Electron Lett 53(2):1655–1657

Khani S, Makki AD, Mousavi SMH et al (2017) Adjustable compact dual-band microstrip bandpass filter using T-shaped resonators. Micro Opt Technol Lett 59(12):2970–2975

Khani S, Mousavi SMH et al (2018) Tunable compact microstrip dual-band bandpass filter with tapered resonators. Microw Opt Technol Lett 60(5):1256–1261

Leu W, Zhang D, Lv D et al (2018) Dual-band microstrip bandpass filter with independently-tunable passbands using patch resonator. Electron Lett 54(10):665–667

Mousavi SMH, Makki SVA et al (2018) Design of a narrow dual-band BPF with an independently-tuanble passband. Electron Lett 54(10):665–667

You B, Chen L, Liang Y et al (2014) A high-selectivity tunable dual-band bandpass filter using stub-loaded stepped-impedance resonators. IEEE Microw Wirel Compon Lett 24(11):736–738